

DIFFRACTION OF WAVES IN COMBUSTIBLE MIXTURES

A. A. Vasil'ev and V. A. Vasil'ev

UDC 534.222.2+536.46+661.215.1

The results of investigations of combustion and detonation wave diffraction, including the nonstationary regimes of combustion–detonation transition, are presented. A wide variety of transient regimes upon diffraction have been revealed. On the basis of diffraction investigations, a criterion of detonation excitation is proposed and formulas for estimating the critical energy of initiation of plane, cylindrical, and spherical waves have been obtained. The calculated values are in good agreement with the experiment.

Keywords: combustion, detonation, combustion–detonation transition, critical diffraction diameter, diffraction reinitiation criterion.

Introduction. As a self-sustained detonation wave (DW) propagates, in the domain of abrupt change in the geometric size of the charge, a complex nonstationary gas-dynamic flow is initiated. This flow received the generalized name diffraction (by analogy with diffraction of the light wave by an obstacle). Diffraction phenomena are characteristic of many problems connected with detonation and shock waves (SW): propagation in channels of varied geometry (divergence, convergence, branching, bends), passage of a DW or an SW through the interface between mixtures (including the passage through an inert gas "lock"), propagation along the free boundary of various combustible systems, upon reflection from obstacles or walls (including profiled ones), etc. It is proper to note that R. I. Soloukhin was one of the first researchers who switched from the three-dimensional investigation of the spherical multifront DW to the simple case of cylindrical symmetry where two parallel planes form a plane gap (channel) of small depth in which the DW propagation belongs with the class of two-dimensional flows.

The previous investigations (beginning with the pioneering works [1–5]) in the classical formulation of a sharply expanding gas charge (the diffraction angle $\alpha = 90^\circ$) showed two qualitatively different modes of wave propagation upon diffraction of the DW depending on the relation between the characteristic size of the initial charge and the characteristic physicochemical scale of the explosive mixture. These modes are as follows (Fig. 1):

1) as soon as the self-sustained DW gets into the expanding region, it begins to be influenced by the convergent rarefaction wave (RW) and always degenerates into a nonstationary complex, including an attenuating shock wave and its accompanying high-speed turbulent flame (DW attenuation);

2) despite the action of the RW, subsequent reinitiation of the divergent DW is always observed.

The regimes between the two modes, when the wave equiprobably (50% to 50%) attenuates or transforms into a divergent DW, are near-critical (also with a probability of any mode lower than 100%).

The second mode represents a convenient experimental method for initiating divergent DWs in combustible mixtures that has found wide use in research laboratories in different countries along with other types of initiators (electric or laser spark, exploding wire, charges of explosives, swift-flying body).

The pulsating multifront character of DWs (unlike the smooth SW front) and the non-one-dimensional gas-dynamic structure of the flow complicated by chemical reactions seriously impede experimental investigations of the DW diffraction, especially of the near-critical regimes of reinitiation. As a consequence, in most experimental works, only the integral parameter of DW diffraction at a diffraction angle $\alpha = 90^\circ$ — the critical parameter d_{**} (e.g., [1–22]) — was determined; the physical aspects of DW diffraction have been studied to a much lesser extent. Acting as a characteristic scale of the gas charge is, for example, the tube diameter d upon transformation of the DW into a quasi-spherical wave ($\nu = 3$) or the channel width l upon transformation of the DW into a quasi-cylindrical wave ($\nu = 2$), and for the characteristic scale of the mixture it is natural to choose the cell size a of the multifront DW. In the case

M. A. Lavrentiyev Institute of Hydrodynamics, Siberian Branch of the Russian Academy of Sciences, 15 Lavrent'ev Ave., Novosibirsk, 630090, Russia, email: gas-det@hydro.nsc.ru. Translated from *Inzhenerno-Fizicheskii Zhurnal*, Vol. 83, No. 6, pp. 1111–1129, November–December, 2010. Original article submitted April 24, 2010.

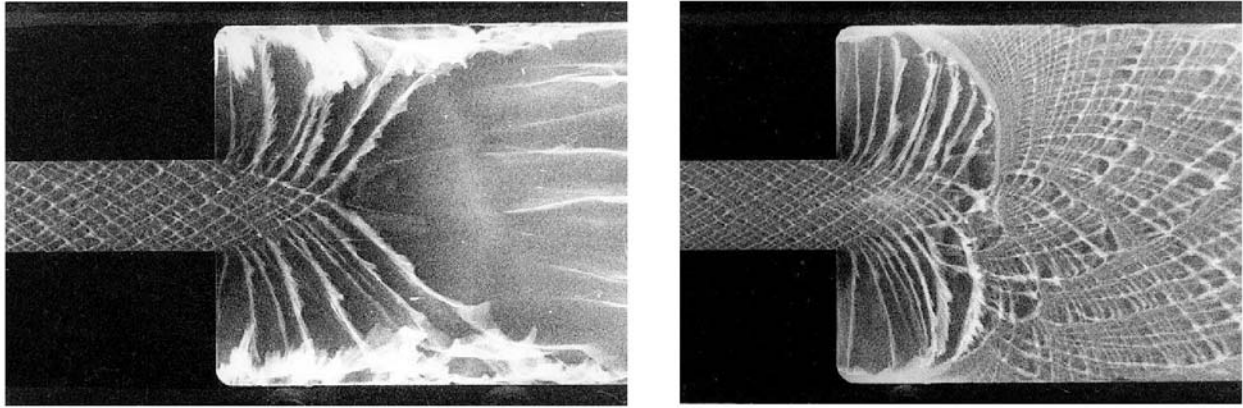


Fig. 1. Photographs of the diffracting DW self-luminescence: on the left — attenuation of the DW and subsequent burning of the mixture by a high-speed turbulent flame; on the right — reinitiation of the divergent DW ($v = 2$).

of a plane channel of critical diameter d_{**} (or critical length l_{**}), the quasi-plane, self-sustained DW equiprobably attenuates or transforms into a divergent DW.

R. I. Soloukhin and V. V. Mitrofanov were the first to formulate the criteria estimate of the DW diffraction in terms of the characteristic size of the detonation cell. On the basis of the available results of experimental investigations of DW diffraction [1–5], the following relations were proposed in [3–5] as a criterion for estimating the critical diameter d_{**} or the critical width of the plane channel l_{**} :

$$d_{**}/a = \text{const} = 13 \quad (v = 3), \quad (1)$$

$$l_{**}/a = \text{const} = 10 \quad (v = 2). \quad (2)$$

Equations of the type (1), (2) were thoroughly tested in numerous subsequent experiments (e.g., in [6–22]) and in the classical scheme of diffraction with $\alpha = 90^\circ$). Such testing was due to not only the scientific interest in DW diffraction as a phenomenon with complex shock-wave interactions, but also the practical applications from the viewpoint of estimating the explosion hazard of combustible systems. In terms of practical applications, the method of diffraction reinitiation of multifront detonation (DRMD) found wide use in laboratory investigations owing to its simplicity compared to other initiators.

A relation of the type (1), (2) is very important in connection with the hypothesis of the key role of the cellular structure in DW initiation and propagation and in connection with the possibility of estimating through a a large number of critical parameters of the multifront DW, namely: initiation energies for various cases of symmetry; geometric sizes of channels for critical propagation of the DW and its transformation in channels of various configurations; size of the swift-flying body capable of exciting a DW in the combustible mixture; critical size of gaseous charge-clouds; coefficients of induction period formulas for the detonation conditions, etc.

Characteristic Schemes of Wave Diffraction. Judging from the number of publications, the case of diffraction with $\alpha = 90^\circ$ has received the most study, while the schemes with $\alpha < 90^\circ$ have been studied to a much lesser extent. Among these are also the numerous schemes of DW propagation in channels of complex geometry: with branching, with bends (smooth or sharp), with perforation of the walls. Among the phenomena that practically have not been studied at all are the diffraction of overcompressed detonation waves, the diffraction of special regimes of detonation (spin, marginal, galloping regimes), the diffraction of quasi-detonation (the quasi-stationary process of wave propagation with a velocity equal approximately to half of the normal detonation velocity), the diffraction of a laminar and a turbulent flame, the diffraction of accelerating flames, including the special case of combustion–detonation transition (CDT). Among the poorly investigated diffraction phenomena are those accompanied additionally, for example, by collisions of the diffracting wave with artificial obstacles or with the nearby lateral walls of a wide channel.

The diffraction angle, the size ratio between the narrow and the wide channels, the degree of overcompression, and many other factors can, under certain conditions, strongly influence the DW reinitiation conditions. Some of the results of such investigations are described in [20], and a review of the state of the art of diffraction problems and results is given in [22]. Recent investigations have shown that relations (1), (2) with constant values of criteria ratios can only be used for approximate estimation; in fact, the values of d_{**}/a and l_{**}/a for various mixtures are not constant and change by a factor of 2, as a minimum, in both directions.

Numerical simulation of the multifront DW diffraction in a non-one-dimensional formulation presents an extremely difficult problem because of the necessity of correct calculation of the phenomena of disappearance of old and initiation of new transverse waves (TW) in a front of diverging multifront detonation. Even at the present time with the availability of powerful multiprocessor computers, only a few programs for calculating the two-dimensional diffraction upon DW divergence are known (e.g., [23–25]). Unfortunately, for example, even the critical value of the parameter d_{**}/a agreeing with experimental data has not yet been calculated.

In the present paper, we have considerably extended the pioneering investigations of R. I. Soloukhin on DW diffraction owing to new formulations and results of investigations of diffraction with the amplitude of the characteristic velocities of propagation of the chemical reaction front in the combustible mixture ranging from centimeters per second (laminar flame) to kilometers per second (detonation, including the strongly overcompressed case).

Experimental Formulation. For diffraction problems, let us make use of the Cartesian coordinate system with the z axis along the direction of wave propagation and the x, y axes in the wave front plane. Consider the case of a spherical DW ($\nu = 3$). For diffraction excitation of spherically diverging waves in the explosion chamber, we used the classical scheme of diffraction: passage of the DW from an initiating tube (IT) of diameter d into an explosion chamber (volume) whose characteristic sizes considerably exceed the tube diameter. In the IT, the wave is quasi-plane, and in the explosion chamber the wave transforms into a spherically diverging wave. Along with the abrupt expansion of the cross section (the diffraction angle $\alpha = 90^\circ$), other schemes (see below) for the case of a cylindrical DW ($\nu = 2$) were used. Diffraction excitation of cylindrically diverging waves was accomplished by two main schemes.

1. The channel was formed as a plane gap of depth Δz between two parallel plates, and the DW was conveyed to the channel through a hole at the center of one of the plates by a rectangular tube whose axis coincided with the channel axis. In so doing, as soon as the DW left the tube and got into the plane gap, it was reflected from the second wall of the gap, i.e., there appeared a higher-pressure region with a characteristic size of the order of the diameter d of the initiating tube whose breakdown (without dynamic upthrust of products) led to the formation of a divergent wave in the gap. Having passed from the tube into the gap, the DW propagated perpendicularly to the z axis as a divergent cylindrical wave (R. I. Soloukhin's scheme).

2. In the plane gap between two parallel plates, a Φ -shaped channel of constant depth Δx was formed and its profile coincided with the profile of the axial cross section of the plant for investigating the diffraction of a spherically divergent wave: the role of the tube and volume diameters is played by the corresponding sizes (width Δy) of the narrow and wide parts of the Φ -shaped channel, and the divergent cylindrical wave was formed in the wide part of the channel. Such plants are called plane channels. Along with Φ -shaped channels, we used P-shaped channels (with diffraction to one side, where the rectilinear wall played the role of the symmetry plane).

Diffraction excitation of the wave corresponding to the plane symmetry ($\nu = 1$) was carried out according to the scheme of formation of two plane channels of equal width Δy joined according to the T-shaped scheme: the DW from one channel (base of T) of depth Δx goes into the perpendicular channel-lintel depth Δz (in the chosen coordinate system), changes the direction of propagation by 90° , and then propagates from the inlet cross section in the form of two divergent plane waves. In so doing, the high-pressure region formed in the channel-lintel by the reflection of the wave of size $(\Delta x) \cdot (\Delta y)$ that has emerged from the channel-base is the initiator for divergent waves in the channel-lintel. It should be borne in mind that for plane symmetry the depth of the initiating channel Δx is a doubled characteristic size of the initiation region upon diffraction to both sides (with respect to the symmetry plane of expansion from the viewpoint of the plane strong explosion model). At one-sided diffraction (Γ -shaped channel), the channel depth coincides with the initial size of the plane initiator.

It will be recalled that in the DRMD method the main problem is the determination of the characteristic sizes of the initiating section (tube diameter d_{**} , "plane" channel width $\Delta = l_{**}$, "plane" slit width Δx_{**}) acting as an equivalent to the critical initiation energy E_* . In the Cartesian coordinate system for cylindrical and plane symmetries,

$\Delta x = h$ plays the role of the plane channel depth, $\Delta y = l$ — that of its width, and the z axis is directed along the axis of the initiating channel. In Soloukhin's scheme for the cylindrically diverging wave ($v = 2$), the role of the thickness of the gap in which the diffracting wave propagates will be played by Δz . For this case, the diagnostic parameters will be d_{**} , Δz , and a . For the plane symmetry, the diagnostic parameters will be the channel depth, the size of the detonation cell, and the size of the initial zone of detonation products Δx , whose breakdown generates quasi-plane diffraction waves (with account for the T- or Γ -shaped diffraction scheme).

Recording. The observed phenomena were recorded by means of pressure cells, high-speed frame-by-frame or scanning schlieren-photography (a high-speed photorecorder optically conjugate with an IAB-461 shadow device), the technique of DW wake prints on sooted foil, and photography of the self-luminescence by the "open shutter" method. Since the DW in combustible mixtures markedly differs from the classical one-dimensional model by its multifront structure, the destruction and recovery of the ordered cellular structure of the DW is an additional indicator that permits obtaining information on the nonstationary processes in the experimental study of the diffraction phenomenon. Note that the propagation of multifront detonation in a channel of small depth is followed by the characteristic diamond-shaped structure of the self-luminescence similar to the structure of wake prints. Both methods of recording cells (wake and self-luminescence) are based on increased parameters of the gas behind the transverse waves of the detonation front: in the wake method higher pressures and in the self-luminescence method higher temperatures are used. It should be particularly emphasized that in the case of mixture combustion the characteristic structure is absent from both the sooted prints and the self-luminescence photographs, which permits easy and unambiguous identification of the detonation and combustion processes.

The main experiments were carried out on mixtures of hydrogen and typical hydrocarbons (acetylene, methane, propane, ethylene) with oxygen and air, as well as on less frequently used fuels such as ammonia, hydrazine, diacine, and synthesis gas. Hydrocarbon fuels have a spectral characteristic convenient for recording — luminescence of the CH radical in the blue spectral region. Moreover, acetylene is known as a very interesting fuel because of the possibility of carbon condensation in reaction products with the formation of nanoparticles, fullerenes, nanotubes, clusters, etc.

The mixture was initiated by a spark discharge by means of a high-voltage generator (electric energy content up to 40 J). Near the initiating electrodes, a vortex generator was located to improve the combustion–detonation transition. The length of the experimental facilities was chosen to be "sufficient" (over 100 calibers) for the formation of a self-sustained wave. Located along the tube were transducers for measuring the DW velocity and its stationarity, the signals from which arrived at the inlets of the frequency meters. Upon its initiation and formation, the self-sustained DW moved from the tube into the explosion chamber — DW diffraction effect. The mixture was allowed to bleed from the side of the explosion chamber. Depending on the initial pressure at a fixed diameter of the tube, the diffraction wave either attenuated or transformed into a spherical DW. In the experiments, we elucidated the critical pressure P_{**} at which in the explosion chamber the processes of excitation or quenching of detonation were observed equiprobably. In investigating the diffraction of fuel–air mixtures (FAM) under laboratory conditions, we used stoichiometric mixtures of acetylene and hydrogen (the least initiation energies). In this case, we used tubes of diameter $d = 80$ and 100 mm as an initiation tube; initiating was accomplished by a blasting cap.

The combustion and detonation parameters of these mixtures in a wide range of concentrations were calculated by the computer program "Bezopastnost'" ("Safety") [26].

Principal Results of the Experiments. The experimental investigations have revealed a wide variety of propagation regimes of combustion and detonation waves both in an initial channel (tube) of constant cross section and upon diffraction.

1. *DW diffraction by the right angle $\alpha = 90^\circ$.* In the classical DW-diffraction scheme [2–4], as the DW passes from a rectilinear tube of constant cross section into a hemispherical volume, for example, in determining the dependence $d_{**}(P_0)$, it was revealed ($d = 2$ –80 mm) that the critical regime of reinitiation is observed at the same pressure P_* of the investigated mixture both in the case of using the classical DRMD scheme with an IT of constant diameter d_{**} (Fig. 2a) and in the case of using a modernized scheme with an IT of larger diameter d_0 in whose outlet cross section thin metal membranes with an axial hole of diameter $d_{**} < d_0$ are located (Fig. 2b). Initiation of a divergent cylindrical wave in a plane channel after the DW leaves the narrow part of the channel of width l and goes into its wide part (both directly or with a membrane) proceeds according to an analogous scheme. This means that the de-

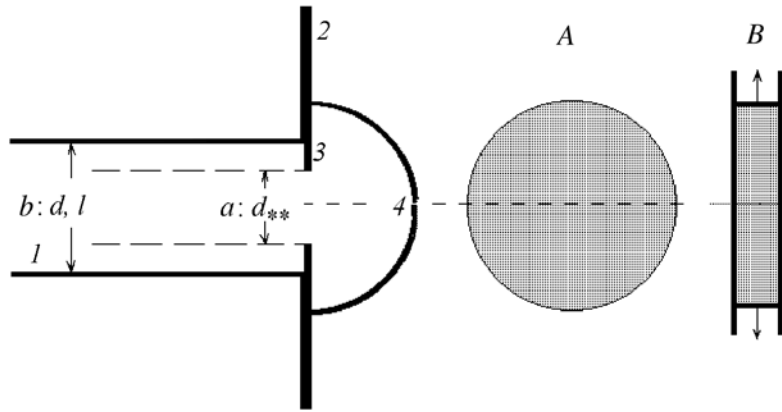


Fig. 2. Scheme of experiments on diffraction initiation of a divergent spherical wave upon the passage of the DW from a tube of diameter d_{**} into the volume (a) or from a tube of diameter $d > d_{**}$ through a membrane with a hole of diameter d_{**} (b): 1) tube or narrow channel; 2) volume or wide channel; 3) membrane with a flow section of a certain form; 4) diffracting divergent wave. On the right — diffracting wave fronts from the side of the axis: A, spherical wave in the volume of $\nu = 3$; B, cylindrical wave in a wide channel of $\nu = 2$ or quasi-plane diffracting wave ($\nu = 1$) excited by the DW going out of a rectangular channel.

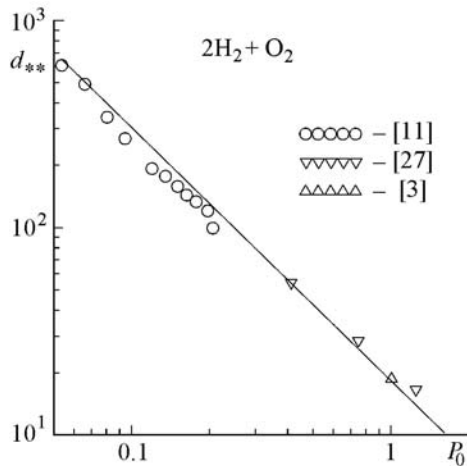


Fig. 3. Critical diffraction diameter depending on the initial pressure ($\nu = 3$). d_{**} , mm; P_0 , atm.

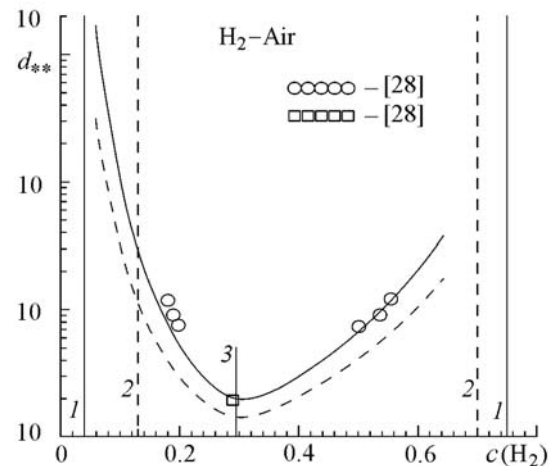


Fig. 4. Critical diffraction diameter depending on the molar concentration of the fuel in the mixture ($\nu = 3$): 1, 2, 3) concentration limits of combustion and detonation and stoichiometric concentration; the solid line shows the calculation [20] and the dashed line — the estimation by the diffraction ratio (1). d_{**} , mm.

termining role in the near-critical initiation is played not by detonation products but by the physical processes directly on the DW front, the most important of which are collisions of transverse waves. The frontal region of the DW in the outlet cross section of the IT having the form of an axially symmetric flat disk acts as an analog of the initiating charge in the DW excitation in a half-space. Under the action of the axially converging unloading wave, this region decreases to zero at a distance from its outlet cross section — at a point that is critical for the subsequent evolution of the process — attenuation or reinitiation. On the basis of the above effect, a "diffraction" method for determining the critical energy of detonation initiation E_{v^*} can be developed (see below).

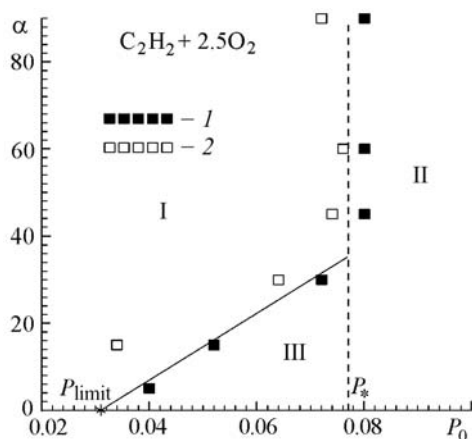


Fig. 5. Critical pressure of diffraction reinitiation at various diffraction angles (passage of the DW from a narrow channel into a wide one, $\nu = 2$): 1) initiation; 2) attenuation; I) region of disruption; II) region of reinitiation, III) region of weakening the disruption phenomena due to the diffraction angle. α , deg; P_0 , P_{limit} , P_* , atm.

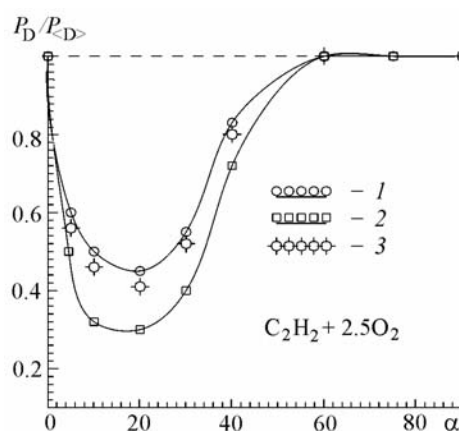


Fig. 6. Critical pressure of diffraction initiation of the mixture by the overcompressed DW normalized to the critical pressure for the self-sustained DW depending on the angle of the cone creating the overcompressed DW: a) $d_{\text{in}} = 100$, $d_{\text{out}} = 30$; 2) 100 and 8; 3) 100 mm and 16 mm. α , deg.

The diagnostic parameters in the scheme of DW diffraction at $\alpha = 90^\circ$ are the critical diameter of diffraction reinitiation d_{**} and the size of the detonation cell a . Figure 3 gives the dependence of d_{**} on the initial pressure of the mixture. Hereinafter, symbols correspond to experimental data and lines — to calculated dependences, abbreviations in the references give the first letters of the authors' names and the year of publication [11, 27, 3]. In Fig. 4, the d_{**} values are given as a function of the molar concentration of the fuel in the mixture (within the concentration limits) in the form of a characteristic U-shaped curve [28]. It is seen that the experimental points are higher than those predicted by (1). Such plots are typical of the majority of fuel–oxygen and fuel–air mixtures (FOM and FAM).

2. *Reinitiation at different diffraction angles.* In investigating the passage of the DW from the IT into the volume through conically diverging nozzles (variation of the diffraction angle $\alpha = 0\text{--}90^\circ$, $d = 8\text{--}40$ mm), it has been established that the quenching phenomena in the diffracting DW intensify as α increases up to some limiting α_* : at $\alpha \geq \alpha_*$ the quenching effects are practically independent of the expansion angle of the detonation front (Fig. 5) (qualitative agreement with the data of [6, 8]). For example, for $\text{C}_2\text{H}_2 + 2.5\text{O}_2$ $\alpha_* \sim 30^\circ$ at $\nu = 3$ and $\alpha_* \sim 45^\circ$ at $\nu = 2$.

3. *Reinitiation of the overcompressed multifront DW.* In investigating the diffraction of the multifront DW in a converging nozzle (overcompression of the wave in a cone with angle α at a fixed inlet diameter $d_{\text{in}} = 100$ mm and a variable outlet diameter $d_{\text{out}} = 8\text{--}20$ mm) with subsequent expansion of the DW (Fig. 6), it has been established that the efficiency of reinitiation of the mixture by an overcompressed wave in the volume is maximum at $\alpha \sim 20^\circ$ and does not differ from the efficiency of the self-sustained DW at $\alpha \approx 0^\circ$ and $\alpha \geq 60^\circ$ due to its weak dependence on the inlet–outlet area ratio characterizing the degree of overcompression of the flow. In Fig. 6, the region below the horizontal dashed line corresponds to a higher efficiency of the overcompressed DW compared to the normal DW. The criteria parameter of reinitiation d_{**}/a in using the overcompressed wave differs from its self-sustained analog in the region of overcompressions β (in velocity) by no more than 10%. As β increases, the critical value of d_{**}/a markedly increases (Fig. 7), which was confirmed independently in [12].

4. *"Chemical" diffraction of the DW.* The "chemical" diffraction of the DW observed in a tube of constant cross section upon the passage of the DW from one mixture to another (gradient of the chemical composition) is typical of the method for determining the concentration limits: the stable DW goes into the investigated mixture and either attenuates (the fuel concentration is beyond the limits) or transforms into a self-sustained DW characteristic of the investigated mixture (within the limits). Some volume of the easy-to-excite mixture near the electrodes is often used as

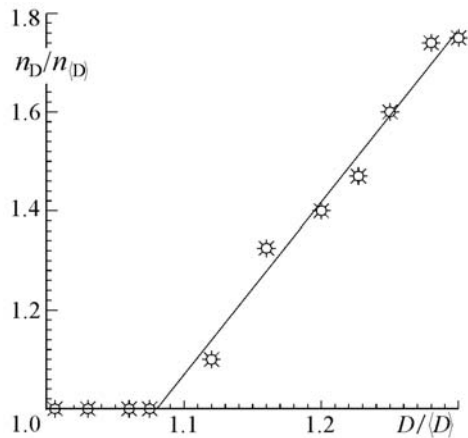


Fig. 7. Number of detonation cells on the outlet cross-section diameter for the overcompressed DW normalized to the analogous number for the self-sustained DW depending on the degree of overcompression of the wave (as to the velocity).

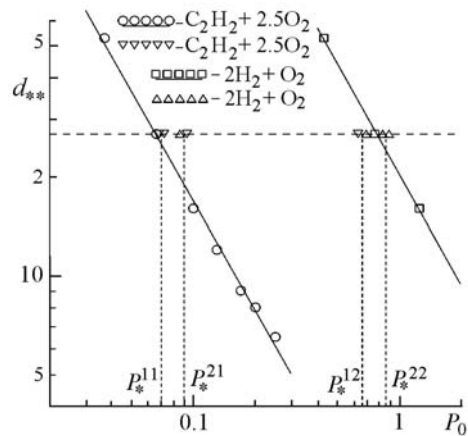


Fig. 8. Critical diffraction diameter ($\nu = 3$) and critical pressure of diffraction initiation for the case where the wave diffracts at the interface between two mixtures: index 1, $C_2H_2 + 2.5O_2$; index 2, $2H_2 + O_2$. d_{**} , mm; P_0 , P_* , atm.

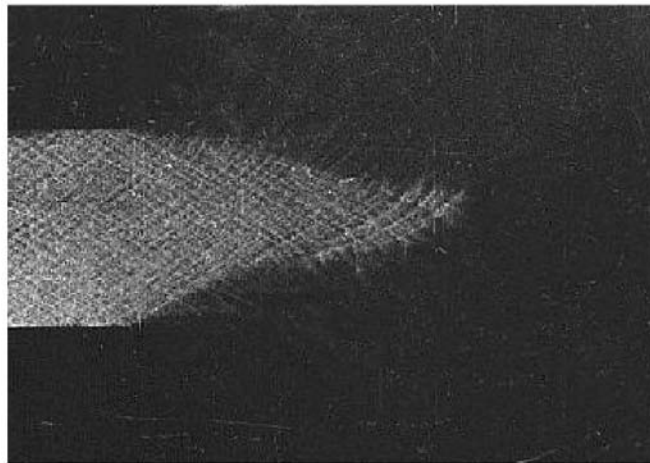


Fig. 9. Photograph of the DW diffraction ($\nu = 2$).

an intermediate initiator for exciting the more difficult-to-excite mixture. The following schemes are varieties of "chemical" diffraction: 1) direct contact between gas charges; 2) charges are separated from each other by an inert interlayer. The latter scheme is well known for condensed explosive charges: detonation transfer through the air space and determination of the safe distance when the second charge will not be able to explode upon unsanctioned explosion of the first one.

The complex variant of "chemical" diffraction where the plane of abrupt expansion of the tube cross section is simultaneously the interface between explosive mixtures differing in activity is not only of practical interest for problems of nonexplosiveness of large volumes of a combustible mixture, but also of more scientific interest for elucidating the role of various processes in the DW reinitiation. For model mixtures, we considered $2H_2 + O_2$ (index 2) and $C_2H_2 + 2.5O_2$ (index 1) mixtures in various combinations (Fig. 8). The results of investigations confirm the concept that the leading role in the reinitiation of multifront detonation is played by collisions of TWs [18].

5. DW diffraction in a mixture with inert dilution. Influence of inert dilution. Figure 9 shows the photograph of the DW attenuation by diffraction, although the number of transverse waves across the channel considerably exceeds the number of waves needed for successful initiation of a cylindrical DW in accordance with criterion (2). This

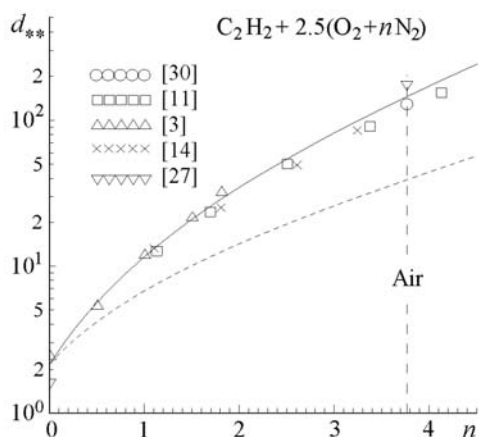


Fig. 10. Critical diffraction diameter ($\nu = 3$) for the mixture diluted with nitrogen (transition from the fuel–oxygen mixture to the fuel–air mixture). The solid line shows the calculation according to [20]; the dashed line shows the calculation according to [29]. d_{**} , mm.

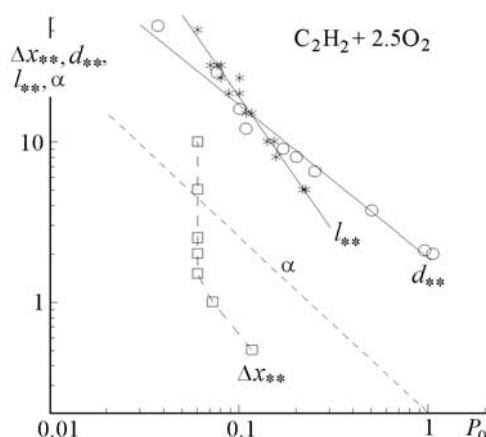


Fig. 11. Critical diffraction scales for spherical d_{**} ($\nu = 3$), cylindrical l_{**} ($\nu = 2$), and plane diffraction Δx_{**} ($\nu = 1$), and the diffraction angle α versus the initial pressure. Δx_{**} , d_{**} , l_{**} , mm. α , deg; P_0 , atm.

photograph illustrates a marked increase in the critical parameter of diffraction l_{**}/a in mixtures highly diluted with argon compared to undiluted mixtures (disturbance of l_{**}/a constancy). Such photographs are observed for various mixtures diluted with argon or helium (by up to 90%). The diffraction experiments have shown that the parameters l_{**}/a and d_{**}/a increase with increasing concentration of the inert gas.

Nitrogen influences the DW in a more complicated manner (Fig. 10). The specific feature of the dependence of the cell size, the critical diffraction parameter, the critical energy of initiation, and other quantities proportional to a on the molar concentration of nitrogen in the mixture is a faster increase in the experimental values with increasing concentration of nitrogen compared to the calculated data obtained under the assumption that the coefficients of the Arrhenius formula for the delay of ignition upon the addition of nitrogen remain unaltered [29]. From Fig. 10 it is seen that the above assumption is evidently violated. This tendency for an increase in the divergence with increasing n is inherent in all fuels and is preserved upon replacing the averaged kinetics equation in the Arrhenius form by the scheme of detailed kinetics with hundreds of elementary reactions. Dilution of mixtures with other inert gases does not lead to such an effect.

One possible explanation of this phenomenon is connected with the increase in the chemical activity of nitrogen under the action of the electric field of the detonation wave that none of the kinetic models takes into account. The second explanation is the illegitimate extrapolation of kinetic constants obtained from combustion experiments to the detonation conditions: first of all, the influence of pressure. It should be emphasized that in many problems nitrogen is still considered to be an inert gas participating in reactions as a third body [30].

6. *Multifront DW.* The natural assumption for shock waves that the diffraction pattern of the cylindrical wave is independent of the channel depth Δx (for $\nu = 2$) is not so obvious for the multifront DW, especially for near-critical regimes. The periodic collisions of TWs at the front responsible for the propagation and reinitiation of the DW are three-dimensional whenever the characteristic sizes of the channel exceed the cell size. One might expect a qualitative change in the characteristics of the diffraction process of the DW in the region of Δx comparable to a when the number of TWs moving in the channel depth (slapping waves on the wake prints) markedly decreases and the TWs propagating in the (y, z) plane remain. In so doing, the following should be borne in mind: although the DW propagation did transform into a two-dimensional one, a marked additional effect on the process of DW diffraction can already be produced by the DW energy and momentum losses caused by the geometric limits of DW propagation in a narrow (in Δx) channel.

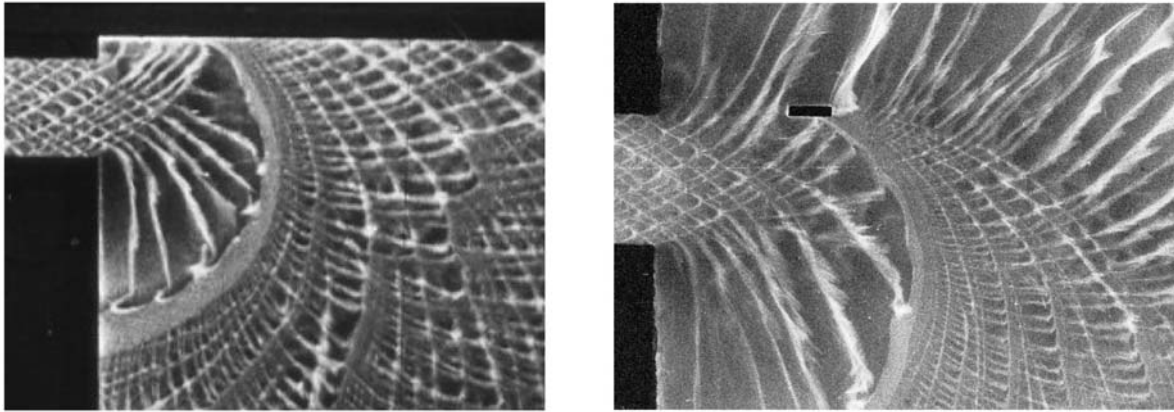


Fig. 12. Reinitiation of the DW ($\nu = 2$) due to the reflection from the nearby lateral wall of a wide channel (left) or from a single obstacle (right).

Investigations of the DW diffraction upon its going from a narrow channel into a wide one ($\nu = 2$) have shown that the critical regimes of initiation depend on both sizes of the initiating (narrow) channel — its width $\Delta y = l$ and height $\Delta x = h$ (the experimental range of Δy and Δx is 2–30 mm). This contradicts the universal character of the ratio l_{**}/a used as a criteria parameter of cylindrical DW reinitiation for numerous mixtures and experimental conditions. The influence of Δx disappears as $h/l \rightarrow 1$, i.e., for the multifront DW, to the strictly cylindrical case of diffraction (independence of the "charge" height by analogy with the "smooth" DW or the shock wave) there correspond experiments with a square cross section of the initiating channel and a minimum value of l_{**}/a . As $h/l \rightarrow 1$ the parameter l_{**}/a increases [20, 31].

7. *Investigation of a plane DW.* Investigations on the plane ($\nu = 1$) initiation (by the DRMD method) have revealed the effect of independence of the processes of multifront DW recovery of the initial pressure of the mixture (Fig. 11) at a size of the initiating gas "lock" Δx_{**} exceeding the size of the detonation wave chemical peak (at a given P_*) [19]. The dependence manifests itself in the case where part of the zone of the DW front that is effective for the initiation is "eaten up"; then, for its compensation, an increase in P_0 is required. For the plane initiation ($\nu = 1$), the diagnostic size is Δx_{**} of the zone occupied by the initiating gas, and the investigations proper are conducted in a channel of constant cross section.

Optimization of the Quenching Phenomena upon Diffraction. The diffracting wave is highly sensitive to artificial reinitiation, for example, due to the interaction with all kinds of "roughnesses" (gaps, ledges) of the experimental equipment (Fig. 12). Due to such an effect, it is possible to considerably weaken the quenching phenomena and increase the probability of DW recovery upon diffraction. Experiments modeling the passage of the DW from a narrow tube d_1 into a wide tube d_2 have shown that the necessary condition for correct determination of d_{**} (or l_{**} for $\nu = 2$) is $d_2 \geq 5d_1$; at smaller d_2 , reinitiation is due to the collision with the lateral wall and is the more effective, the smaller the difference between d_1 and d_2 ($d_1 = 5\text{--}60$ mm, d_2 is up to 250 mm). The ratio d_1/d_2 serves as an additional parameter of the given problem. A consequence of the artificial reinitiation is the underestimation of the critical diffraction parameters.

The quenching phenomena noticeably weaken with decreasing diffraction angle ($\alpha \ll \alpha_*$). The limiting case is the diffraction by a curvilinear surface smoothly joined with the walls of the main channel. Upon diffraction by a curvilinear surface, the diagnostic parameters are the width $\Delta y = l_{**}$ and depth Δx of the channel, as well as the boundary surface equation $y = y(z)$. For a boundary in the form of a circular sector, the radius R becomes a diagnostic parameter instead of the dependence $y = y(z)$. The photographs of the self-luminescence upon DW diffraction by a curvilinear surface smoothly joined with the channel wall with breaking and reinitiation of a multifront DW are shown in Fig. 13. The points A mark the reinitiation centers in an expanding wave. The reinitiation conditions are determined by the ratio between the radius of curvature of the surface R and the initial channel width l . The qualitative laws are analogous to the case of diffraction by a rectilinear surface — the role of the expansion angle α is now played by the parameter R/l .

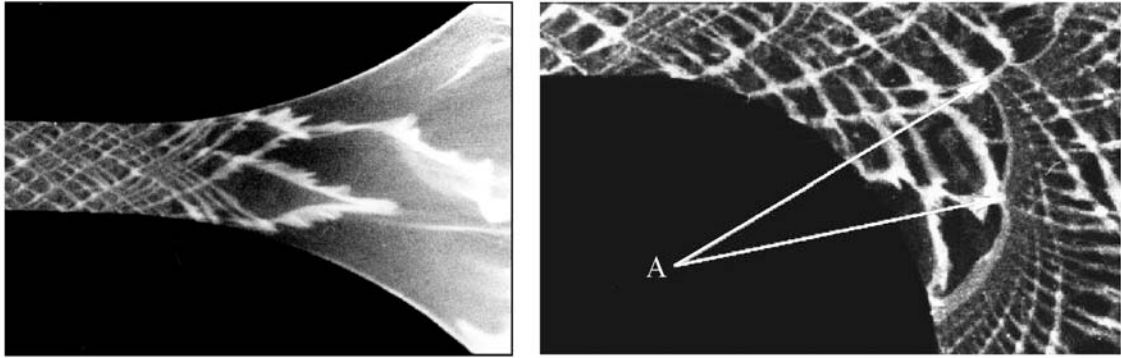


Fig. 13. Photograph of the diffraction by a curvilinear surface: on the left — attenuation; on the right — reinitiation of the DW.

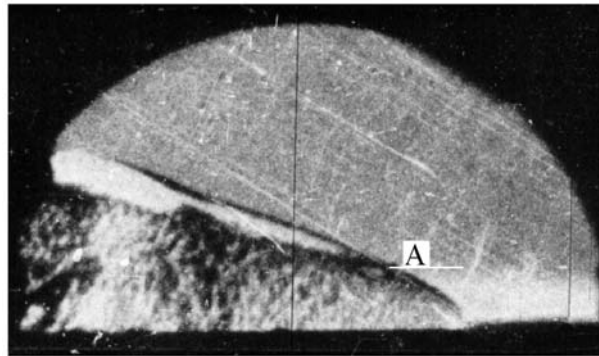


Fig. 14. Diffraction of the DW propagating along the layer of the combustible mixture (the bar under the base of the letter A marks the mixture–air interface).

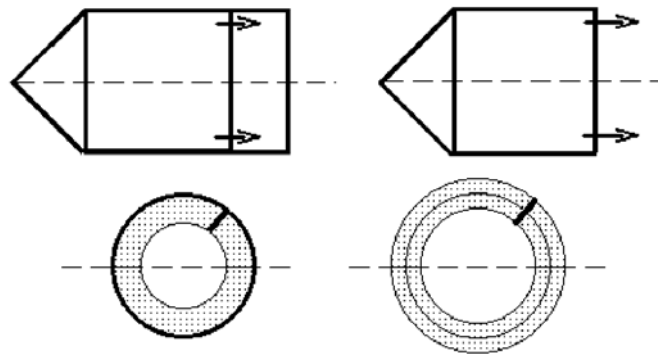


Fig. 15. Idealized scheme of generation of an annular jet bounded by an outer rigid wall (on the left) or a free jet (on the right).

Among the diffraction problems are problems on the DW propagation along charges having no bounding walls (Fig. 14) — a jet or a layer of the combustible mixture (submerged or in a cocurrent flow) [32]. For a free charge-jet, the most important parameter is the critical detonation diameter d_{*} , and for a charge in the form of a flat layer with a cross section $x \cdot y$ and $y \gg x$ — the critical thickness of the layer $\Delta x = h_{*}$. Of particular interest are gas charges in the form of an annular jet, for example, when the fuel is injected through nozzles mounted around the circumference (Fig. 15, external combustion model) [33]. For the latter case, the diagnostic parameters will be the radius of the inner boundary and the thickness of the ring layer of the combustible mixture. The possibility of experimental realization of external burning of the mixture in the detonation regime is illustrated by the photograph in Fig. 16. In the given scheme of detonation burning of the mixture in a rotating wave, it is easy to isolate hot reaction products from direct contact with the lateral walls of the combustion chamber and thus considerably decrease the thermal load

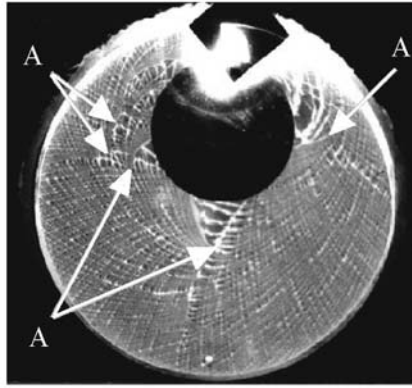


Fig. 16. Photograph of the self-luminescence illustrating the possibility of detonation burning of the mixture in a free jet by means of a rotating DW (external detonation combustion).

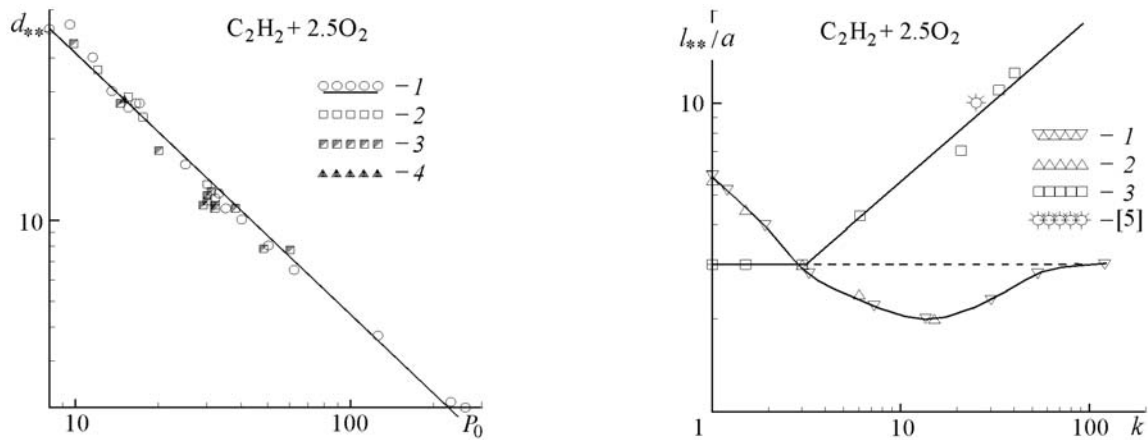


Fig. 17. Effective critical diffraction diameter ($\nu = 3$) versus the initial pressure of charges in the form of a circle (1), a square (2), a regular polygon (3), and a triangle (4). d_{***} , mm; P_0 , atm.

Fig. 18. Criterion of diffraction initiation of a cylindrical DW versus the width-length ratio of the rectangular charge: 1) set of experiments on the excitation of a spherical DW by rectangular charges of equal area; 2) set of experiments on the excitation of a spherical DW by rectangular charges with a variable width and a constant length; 3) set of experiments on the excitation of a cylindrical DW by rectangular charges with a variable width and a constant length.

on the engine and increase the degree of conversion of thermal (internal) energy of detonation products to kinetic energy of outflowing gases.

In axisymmetric initiation (equivalent plane charges in the form of an ellipse, a square, a regular triangle, a rectangle, etc.), the diagnostic parameters are the minor and major axes of the ellipse, the side of the square or triangle, and the length and width of the rectangular charge [16, 17, 20]. For the conditions of axisymmetric initiators, the effective critical diameter is determined as a geometric mean of the diameters of the inscribed and circumscribed circles $d_{***} = \sqrt{d_{1*} \cdot d_{2*}}$. The experimental results are presented in Fig. 17.

The transformation of the charge form from circular (diameter d) through square to rectangular (length H , width L) in the classical diffraction scheme (passage of the DW into the volume) makes it possible to switch from the initiation of a spherical DW (charge-circle) to the initiation of a cylindrical DW (charge-thread of rectangular cross section at $H/L \gg 1$) and determine the ratios between the sizes of d_{***} and l_{***} characteristic of these symmetries. For

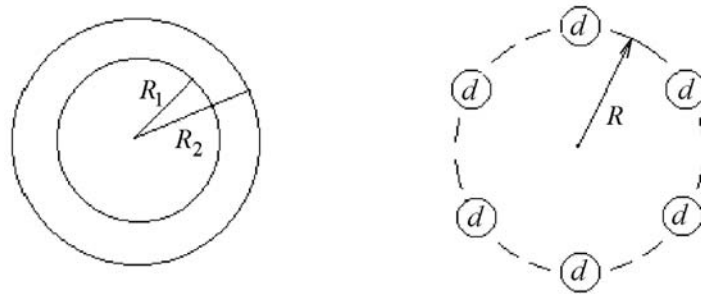


Fig. 19. Scheme optimizing the diffraction reinitiation of the DW by changing the configuration of the initiating charge: ring charge, multicharge (multipoint) scheme.

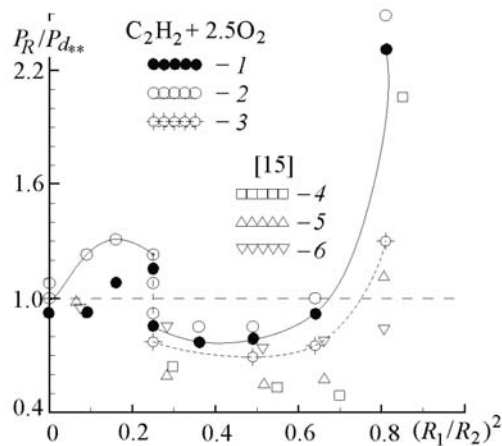


Fig. 20. Mixture pressure at a critical initiation of a DW by ring charges (normalized to the corresponding value for the continuous charge) versus the ratio between the ring radii: 1, 2) attenuation and reinitiation of the DW for $R_2 = 15$ mm; 3) reinitiation at $R_2 = 20$ mm; 4–6) data [15] for the mixtures C_2H_2 — air (stoichiometry), $C_2H_2 + 2.5O_2$, $C_2H_2 + 2.5O_2 + 10.5Ar$, respectively.

the charge-thread in the ideal case, the cylindrical character of the excited-wave propagation is preserved in any gap formed by two parallel planes perpendicular to the thread axis. The charge length H therewith is an analog of the diffraction channel depth h , and the charge width L is an analog of the channel width l . An analogous dependence can also be investigated on plane channels by varying the width–depth ratio of the channel $k = l/h$. Figure 18 graphically represents the critical conditions for diffraction initiation of cylindrical detonation as a function of k . The asterisk shows the result of [5] obtained in a channel of size 25×1 mm ($k = 25$) that served as the basis for relation (2) for cylindrical symmetry. It is seen that the result of [5] perfectly falls on the experimental curve but evidently disagrees with relation (2) for (l_{**}/a) as a universal criteria parameter of the cylindrical DW reinitiation for various mixtures and experimental conditions.

For the ring initiator, the diagnostic parameters are the inner R_1 and outer R_2 radii of the charge (Fig. 19) and the size of the detonation cell a [23–25]. As a result of the investigations, it has been found that between R_1 , R_2 , and a there exists a relation at which the efficiency of the ring initiator is an order of magnitude higher compared to the initiator in the form of a solid disk. In Fig. 20, the region below the horizontal dashed line corresponds to the higher efficiency.

In the scheme of multipoint initiation, the diagnostic parameters are the number of individual microinitiators N with a characteristic size of d and their spatial arrangement relative to one another [17, 20]. The basic laws are similar to the case of the ring charge: the efficiency of the multipoint scheme can exceed many times the efficiency of the initiator in the form of a solid disk. Figure 21 shows two typical photographs of the observed phenomena. The left photograph shows the diffraction of a flame. This photograph clearly demonstrates the role of the spatial distribu-

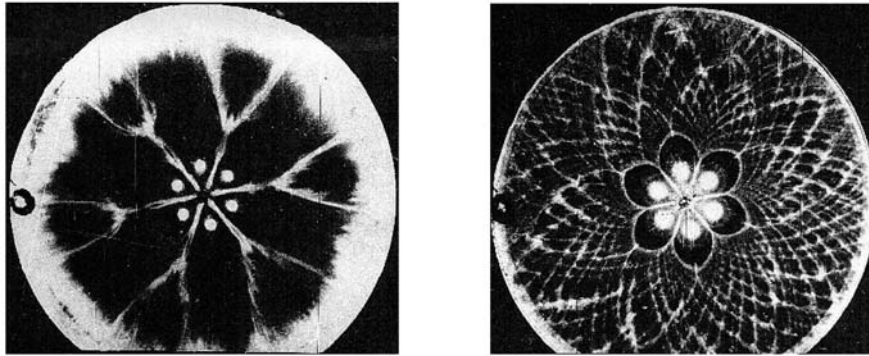


Fig. 21. Photographs of the multifront excitation of combustion and detonation in the mixture ($\nu = 2$) with an efficiency considerably exceeding (by an order of magnitude) the effect of a single charge of the total mass (energy).

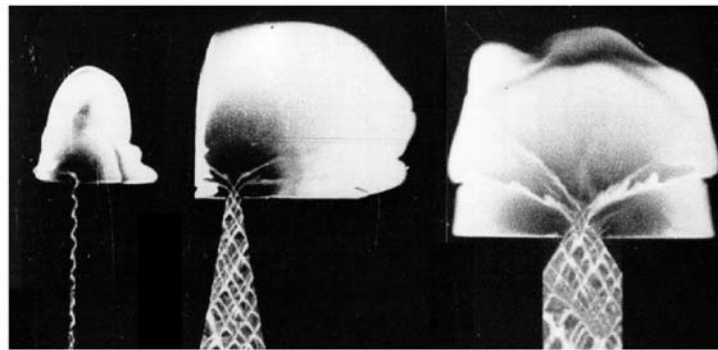


Fig. 22. Effect of complete breaking of detonation and combustion waves by the diffraction for the near-limiting detonation (on the left) and the overcompressed DW (in the middle and on the right).

tion of ignition sources when not only the sources themselves but also the regions of interaction of combustion fronts from adjacent igniters play an important part in the mixture initiation. A characteristic feature of this photograph is the bifurcation of the collision line of the fronts from adjacent igniters — the "wine-glass-shaped" structure (change-over from regular collision to irregular (Mach) collision). The right-hand photograph shows the pattern of successful excitation of detonation with the aid of a distributed multipoint excitation scheme for the conditions where the concentrated initiator with an energy equivalent to the multipoint scheme fails to initiate a DW (the efficiency of the multicharge scheme is higher than that of the concentrated scheme).

In all the cases considered above, the initiating quasi-plane DW was multifront. Of particular interest is the near-limiting DW with a small number of TWs on the front. Investigations of the near-limiting DW diffraction have revealed such a phenomenon as not only quenching of detonation by diffraction but also even flame-out in the expanding wave that shows up as complete disappearance of the luminescence of products (photographs in Fig. 22). In so doing, the flame-out effects are observed not only for the self-sustained DW but also for the overcompressed one. The nature of this effect requires additional studies.

The nontraditional behavior of the wave upon flame diffraction is illustrated in two photographs (Fig. 23): initiation of detonation in a wide channel upon flame expansion. Such a situation is realized in the case where the CDT point is situated near the diffraction cross section. The latter can be provided by varying the initiator energy (the critical ignition energy of the mixture is always much lower (by a few orders of magnitude) than the critical initiation energy of the DW), the mixture composition, the initial pressure, the length of the initiation section, etc. The DW initiation upon flame diffraction is of particular interest, since upon CDT the highest possible pressures that are much higher than the pressure of products of the self-sustained DW are realized (due to the strong overcompression of the DW). About half a century ago, in [34] the CDT near a closed end of a tube (due to the variation of the mixture

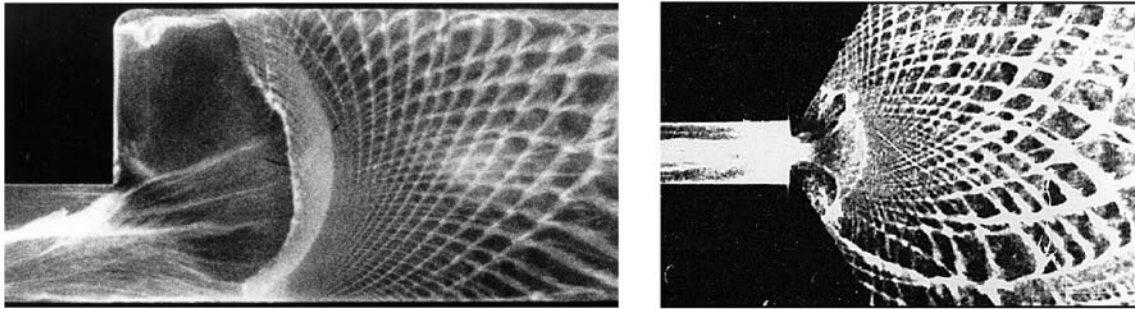


Fig. 23. CDT (flame diffraction, $\alpha = 90^\circ$) due to the reflection of the rarefaction wave from the axial wall (on the left) and CDT due to the passage of the flame through the nozzle into the divergent channel (on the right).

composition) caused a metal wall of thickness 10 mm to collapse! A very dangerous situation that cannot be ignored in modeling the initiation and development of emergency nucleation site of the flame in a space with various kinds of obstacles. From another point of view, having learned to control the position of the CDT point, we obtain a highly effective method for optimizing the initiation processes.

The nontraditional influence of the combustion–detonation transition near the diffraction cross section is evidenced by Fig. 24, presenting the critical pressure P_* of the $12\text{C}_2\text{N}_2 + 13\text{O}_2$ mixture (close to equimolar) for successful reinitiation of the DW by diffraction (passage from a tube of diameter $d = 6$ mm into a tube with $d = 44$ mm) depending on the length L of the initiating section of the tube. It can be seen that at $L > 400$ mm the conditions for diffraction reinitiation do not depend on the length of the initial section. This is explained by the fact that the CDT point is localized in the initiating section before the diffraction cross section, and in this case the normal DW diffracts. But at $L < 400$ mm an unusual behavior is observed — successful diffraction reinitiation of the DW at a lower pressure with some optimal value of P_* . The U-shaped region in Fig. 24 corresponds to the higher efficiency. The nature of this effect is connected with the approach of the diffraction cross section (variation of the length) immediately to the CDT point, and the powerful wave from the CDT automatically provides DW reinitiation not only at a given pressure but also at a lower pressure. But when the CDT point "gets" into depths far from the diffraction cross section and recedes from the optimal position, then, to reinitiate the DW, it is necessary to increase the pressure from P_* again.

It should be especially emphasized that the nontraditional regimes of diffraction investigated in the present paper represent good test material for future numerical simulation. Such simulation has not yet been realized.

Critical Initiation Energy. The determination of the critical energy of initiation E_* is one of the most important detonation problems that is of scientific and applied importance (ecology and non-explosiveness). At present, about 20 approximate approaches to the estimation of E_* are known. The most comprehensive analysis of the known methods for estimating E_* , the correlation between estimates, and the agreement between calculated and experimental data are given in [20, 35]. The main conclusion is as follows: the E_* values calculated by the existing models differ by several orders of magnitude, and the set of published experimental data on the initiation with least deviations is yielded by the "surface energy" model presented in [36] and the model of multipoint initiation (MPI) of [10, 37] (preliminary investigations by the multipoint model were conducted in [38–39].)

The increase in the number of analyzed estimates did not affect the independent conclusion [36] about priority of the "surface energy" and multipoint initiation models when the estimation proposed in [40] is added to [36, 37]. Nevertheless, even the "best" models at equal kinetic constants yield a spread of calculated E_* values differing by severalfold. For example, for the initiation of a spherical DW in a stoichiometric hydrogen–air mixture, $E_* \approx 4.5 \cdot 10^2$ J calculated by the formulas of [36], $E_* \approx 1.4 \cdot 10^3$ J in accordance with [40], and $E_* \approx 3.2 \cdot 10^3$ J obtained by the formulas of the multipoint initiation model. Therefore, new approaches to the refinement of E_* are still urgent, especially for practical use.

In all approximate (and, as a rule, one-dimensional) approaches, by a particular technique, first the value of the parameter most critical for the formation of a detonation wave is determined — the initiating wave amplitude, the duration of its action, the characteristic radius of the wave, the size or period of the induction zone, etc. In using such a critical parameter, the initiation energy E_* is recalculated. For diverging waves, the one-dimensionality condition per-

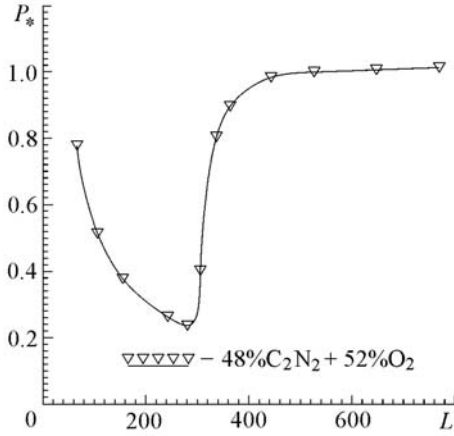


Fig. 24. Critical pressure of CDT diffraction ($\nu = 3$) versus the length of the initiating tube (influence of the CDT point on the reinitiation of the DW in the volume). P_* , atm; L , mm.

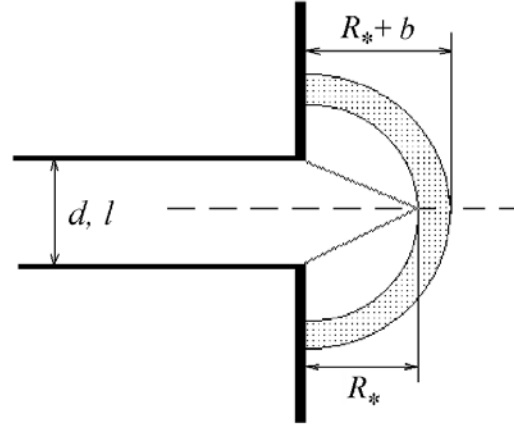


Fig. 25. Idealized scheme of the critical layer of the mixture upon diffraction initiation of a DW.

mits following the initiation dynamics along a certain direction or within the limits of a tube of current taken separately. In the present paper, the choice of the critical parameter of initiation is made on the basis of the phenomenon of DW diffraction by a right angle.

For the critical parameter for DW reinitiation by diffraction, we chose the radius of the diffracting wave at the instant of time at which the axial rarefaction wave reaches the charge axis, disturbing the chemical reaction behind the DW front as it propagates over the DW front from flanks to the axis (Fig. 25). Points R_{3*} are critical for the DW reinitiation. It is here that the course of subsequent events is determined and it is here that the energy of the external initiator is important. The value of this energy should be such that the insufficient chemical release of energy be compensated and the DW be recovered on the b scale characteristic of the self-sustained regime of DW propagation. At lower initiator energies the DW will not be recovered and the process will be disturbed.

On the basis of the diffraction phenomenon the criterion of detonation excitation has been formulated as follows: the critical energy of initiation should exceed the work of expansion of detonation products throughout a layer of thickness b counted from the critical point:

$$E_{3*} = \int_{R_{3*}}^{R_{3*}+b} P_{CJ} 4\pi r^2 dr = 4\pi P_{CJ} (3R_{3*}^2 b + 3R_{3*} b^2 + b^3) / 3 \approx \rho_0 D_0^2 b^3 4\pi \pi_{CJ} \left[2.4 \tan^2 \varphi (d_{**}/a)^2 + 2.7 \tan \varphi \cdot d_{**}/a + 1 \right] / \gamma_0 M_0^2 = B_3 \rho_0 D_0^2 b^3, \quad (3)$$

$$E_{2*} = \int_{R_{2*}}^{R_{2*}+b} P_{CJ} 2\pi r dr = \pi P_{CJ} (2R_{2*} b + b^2) \approx \rho_0 D_0^2 b^2 \pi \pi_{CJ} \left[1.8 \tan \varphi (l_{**}/a) + 1 \right] / \gamma_0 M_0^2 = B_2 \rho_0 D_0^2 b^2, \quad (4)$$

$$E_{1*} = \int_{R_{1*}}^{R_{1*}+b} P_{CJ} dr = P_{CJ} b \approx \rho_0 D_0^2 b \pi_{CJ} / \gamma_0 M_0^2 = B_1 \rho_0 D_0^2 b, \quad (5)$$

where $\tan \varphi = a/b$ and E_* is independent of R_{1*} . The general formula has the form

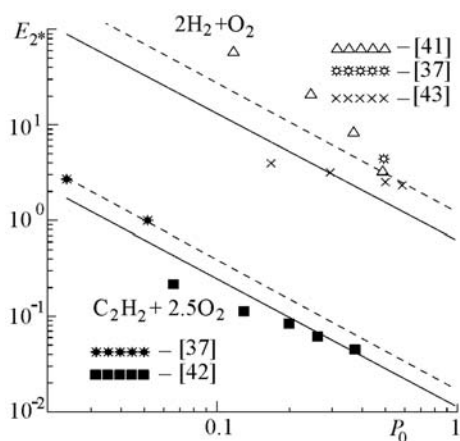


Fig. 26. Critical energy of cylindrical DW initiation versus the initial pressure for stoichiometric mixtures of hydrogen and acetylene with oxygen. The solid lines show the calculations by the multipoint initiation model (1), the dashed lines — by the diffraction initiation model (2). E_{2*} , J; P_0 , atm.

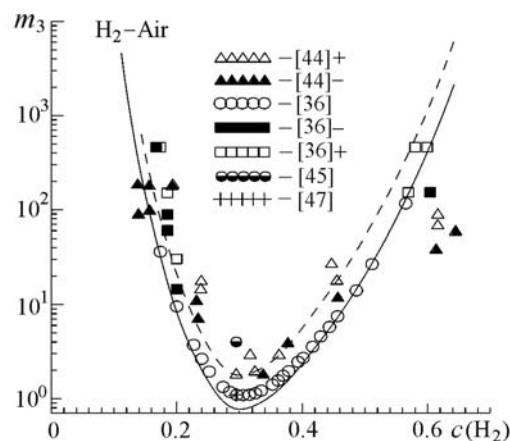


Fig. 27. Critical mass of the trotyl charge for initiating a spherical DW in hydrogen–air mixtures versus the molar concentration of hydrogen in the mixture. The solid lines show the calculations by the multipoint initiation model (1), the dashed lines — by the diffraction initiation model (2); the signs + (plus) and – (minus) mark the regimes of excitation and attenuation of the DW. m_{ch} , g; $c(\text{H}_2)$, mole/ m^3 .

$$E_{v*} = B_v \rho_0 D_0^2 b^v.$$

Figures 26 and 27 present the experimental data on the critical energy of initiation of a cylindrical DW and the critical mass of the trotyl charge needed to initiate a spherical DW from [20, 41–47] and the corresponding calculated data obtained with the use of the models of multipoint and diffraction initiation. It is seen that both models predict fairly well the values of the critical energies of initiation of gaseous mixtures. The data presented in Fig. 27 illustrate the comparative efficiency of initiation of various mixtures (safety problem). It should be emphasized that the choice of the quantity R_{v*} as a diagnostic scale makes it possible not to consider the internal multifront DW structure in terms of the diffraction estimate (as in the model of multipoint initiation) and remain within the framework of one-dimensional representations of the DW.

Conclusions. We have conducted experimental investigations of the diffraction of combustion and detonation waves in various fuel–oxygen and fuel–air mixtures with a wide variation of their basic geometric, gas-dynamic, and physicochemical parameters (pressure, fuel–oxidizer ratio, degree of dilution with inert gases, degree of overcompression).

The new experimental formulations have revealed a wide variety of propagation regimes of combustion and detonation waves upon diffraction.

The main parameters responsible for the wave diffraction have been revealed. It has been shown that the classical criteria in the form of a constant ratio between the characteristic geometric size of the experimental equipment and the characteristic size of the detonation cell (as the main scale of the combustible mixture) can be used for approximate estimations. Actually, these quantities can reach a twofold deviation (in both directions) for various mixtures, especially at a high dilution and a strong overcompression.

The reinitiation efficiency can be increased and optimized by many techniques: by changing the symmetry type, using ring initiators, and reflection from the walls. At an optimal ratio between the spatial-temporal characteristics of the initiator and the combustible mixture, the critical energy of initiation can be decreased by orders of magnitude.

Control of the combustion–detonation transition points represents a highly effective method for optimizing the initiation processes.

This work was supported by the Russian Foundation for Basic Research (grant 08-01-00347), the leading scientific school of the RF "Mechanics of shock and detonation processes," and the RAS Program "Fundamental principles of energy technologies, including the VTSR."

NOTATION

a , b , transverse and longitudinal sizes of the detonation cell, mm; B_v , proportionality coefficient in the formula for the critical energy of initiation depending on the symmetry type; $c(\text{H}_2)$, molar concentration of the fuel in the mixture, mole/m³; d , d_0 , diameters of the initiating tube, mm; d_1 , d_2 , diameters of tubes in the scheme of DW passage from the narrow part to the wide part, mm; d_{1*} , d_{2*} , diameters of the inscribed and circumscribed circles for charges in the form of an ellipse, a square, and a regular polygon, mm; d_* , critical diameter of detonation (minimal diameter of the cylindrical charge without a shell for the self-sustained regime of DW propagation), mm; d_{**} , critical diameter of diffraction, mm; D , wave velocity, m/s; $\langle D \rangle$, velocity of the self-sustained DW, m/s; D_0 , velocity of the ideal Chapman–Jouguet DW (without losses), m/s; E_* , critical energy of initiation, J; E_v^* , critical energy of initiation for the corresponding symmetry type, J ($v = 3$); J/cm ($v = 2$); J/cm² ($v = 1$); $h = \Delta x$, depth of the diffraction channel, mm; $k = l/h$, ratio between the sides of the rectangular channel; $l = \Delta y$, width of the diffraction channel, mm; l_{**} , critical width of the diffraction channel, mm; L_* , distance from the ignition point to the CDT point (CDT length), mm; L , H , width and length of the rectangular charge, mm; M_0 , Mach number of the Chapman–Jouguet DW; m_{ch} , charge mass, g; N , number of initiators in the multipoint scheme; n , nitrogen–oxygen ratio ($n = 3.76$ for air); n_D , criteria number for diffraction of the overcompressed wave; $n_{\langle D \rangle}$, criteria number for diffraction of the self-sustained wave; P_0 , initial pressure, atm; P_{CJ} , pressure of Chapman–Jouguet detonation products, atm; P^{11} , P^{12} , P^{21} , P^{22} , critical pressures of diffraction initiation at the interface between two mixtures: $\text{C}_2\text{H}_2 + 2.5\text{O}_2$ (index 1) and $2\text{H}_2 + \text{O}_2$ (index 2); P_* , critical pressure of diffraction reinitiation, atm; P_D , critical pressure of overcompressed DW diffraction, atm; $P_{\langle D \rangle}$, critical pressure of self-sustained DW diffraction, atm; P_{limit} , limiting pressure of the existence of a self-sustained DW, atm; $P_{d_{**}}$, critical pressure of continuous charge diffraction, atm; P_R , critical pressure of ring charge diffraction, atm; R , radius of curvature, mm; R_1 , R_2 , ring charge radii, mm; R_v^* , diffracting-wave radius at the moment of convergence of rarefaction waves on the charge axis chosen as a critical radius of diffraction initiation of the mixture, mm; r , coordinate; x , y , z , Cartesian coordinate axes; Δx , Δy , Δz , ranges of change, mm; Δx_{**} , critical size of the diffraction region for the plane DW, mm; α , angle of initial diffraction (angle of deviation of the charge boundary from the axial direction), deg; α_* , limiting angle of influence on DW diffraction, deg; β , degree of overcompression (velocity ratio between the overcompressed wave and the self-sustained wave); γ_0 , adiabatic index of the investigated mixture; v , index of symmetry ($v = 1, 2, 3$ for the flat, cylindrical, and spherical cases); ρ_0 , density of the investigated mixtures, kg/m³; $\pi = 3.14$, constant; $\pi_{\text{CJ}} = P_{\text{CJ}}/P_0$; φ , angle of the trajectories of transverse waves with the axis of DW propagation, $\tan \varphi = a/b$.

REFERENCES

1. C. Campbell, The propagation of explosion waves in gases contained in tubes of varying cross-section, *J. Chem. Soc.*, 2483–2498 (1922).
2. P. Laffitte, On the propagation of a spherical explosion wave, *Com.-Rend. Acad. Sci.*, **177**, 178–180 (1923).
3. Ya. B. Zel'dovich, S. M. Kogarko, and N. N. Simonov, Experimental investigation of the spherical gas detonation, *Zh. Tekh. Fiz.*, **26**, No. 8, 1744–1768 (1956).
4. B. V. Voitsekhovskii, V. V. Mitrofanov, and M. E. Topchiyan, *Structure of the Detonation Front in Gases* [in Russian], Izd. SO AN SSSR, Novosibirsk (1963).
5. V. V. Mitrofanov and R. I. Soloukhin, On the multifront detonation wave diffraction, *Dokl. Akad. Nauk SSSR*, **159**, No. 5, 1003–1006 (1964).
6. S. M. Kogarko, On the possibility of detonation of gaseous mixtures in conical tubes, *Izv. Akad. Nauk SSSR, OKhN*, No. 4, 419–426 (1956).
7. R. A. Strehlow, A. A. Adamczyk, and R. J. Stiles, Transient studies of detonation waves, *Acta Astronaut.*, **17**, Nos. 4–5, 509–527 (1972).

8. R. A. Strehlow and R. J. Salm, The failure of marginal detonations in expanding channels, *Acta Astronaut.*, **3**, No. 11, 983–994 (1976).
9. D. H. Edwards, G. O. Thomas, and M. A. Nettleton, The diffraction of a planar detonation wave at an abrupt area change, *J. Fluid Mech.*, **95**, No. 1, 79–96 (1979).
10. A. A. Vasil'ev and V. V. Grigor'ev, Critical conditions of propagation of gas detonation in sharply expanding channels, *Fiz. Goreniya Vzryva*, **16**, No. 5, 117–125 (1980).
11. R. Knystautas, J. H. Lee, and C. M. Guirao, The critical tube diameter for detonation failure in hydrocarbon-air mixtures, *Combust. Flame*, **48**, 63–83 (1982).
12. D. Desbordes and M. Vachon, Critical diameter of diffraction for strong plane detonations, in: J. R. Bowen, J.-C. Leyer, and R. I. Soloukhin (Eds.), *Dynamics of Explosion; Progress in Astronautics and Aeronautics*, Vol. 106, New York (1986), pp. 131–143.
13. W. B. Benedick, R. Knystautas, and J. H. Lee, Large-scale experiments on the transmission of fuel-air detonations from two-dimensional channels, in: J. R. Bowen, N. Manson, A. K. Oppenheim and R. I. Soloukhin (Eds.), *Dynamics of Shock Waves, Explosions and Detonations; Progress in Astronautics and Aeronautics*, Vol. 94, New York (1983), pp. 546–556.
14. Y. K. Liu, J. H. Lee, and R. Knystautas, Effect of geometry on the transmission of detonation through an orifice, *Combust. Flame*, **56**, 215–225 (1984).
15. J. O. Moen, A. Sulmistras, J. Thomas, et al., The influence of cellular regularity on the behavior of gaseous detonations, in: J. R. Bowen, J.-C. Leyer, and R. I. Soloukhin (Eds.), *Dynamics of Explosion; Progress in Astronautics and Aeronautics*, Vol. 106, New York (1986), pp. 220–243.
16. A. A. Vasil'ev, Initiation of gas detonation in the case of spatial distribution of sources, *Fiz. Goreniya Vzryva*, **24**, No. 2, 118–124 (1988).
17. A. A. Vasil'ev, Spatial excitation of multifront detonation, *Fiz. Goreniya Vzryva*, **25**, No. 1, 113–119 (1989).
18. A. A. Vasil'ev, Propagation of gas detonation at a simultaneous change in the tube cross-section and mixture composition, *Fiz. Goreniya Vzryva*, **20**, No. 6, 142–147 (1984).
19. N. V. Bannikov and A. A. Vasil'ev, Plane initiation of detonation, *Fiz. Goreniya Vzryva*, **29**, No. 3, 164–170 (1993).
20. A. A. Vasil'ev, *Near-Critical Regimes of Gas Detonation*, Doctoral Dissertation (in Physics and Mathematics), Novosibirsk (1995).
21. A. A. Vasil'ev, Modes of a detonation and high-speed burning in channels with perforated walls, in: V. Molkov (Ed.), *Fire-and-Explosion Hazard of Substances and Venting of Deflagrations — Proc. 2nd Int. Seminar*, All-Russia Research Institute for Fire Protection, Moscow (1998), pp. 582–592.
22. A. A. Vasil'ev et al., The basic results of reinitiation processes in diffracting multifront detonations. Part I, *Eurasian Chem.-Technol. J.*, **5**, No. 4, 279–289 (2003).
23. K. Hiramatsu, T. Fujiwara, and S. Taki, A computational study of transmission of gaseous detonation to unconfined space, in: *Proc. 20th Int. Symp. on Combust.*, Pittsburgh (1984).
24. M. Fisher, E. Pantow, and T. Kratzel, Propagation, decay and re-ignition of detonations in technical structures, in: G. Roy, S. Frolov, K. Kailasanath, and N. Smirnov (Eds.), *Gaseous and Heterogeneous Detonations. Science to Applications*, ENAS Publishers, M., (1999), pp. 197–212.
25. B. Khasainov, C. Priault, H.-N. Presles, and D. Desbordes, On the mechanism of transition of self-sustained detonation from a tube to a half-space through an annular orifice with a central obstacle, in: *Proc. 18th Int. Colloq. on the Dynamics of Explosions and Reactive Systems*, July 29–August 3, 2001, Seattle, USA, University Washington, CD ISBN 0-9711740-0-8. N. 096.
26. A. A. Vasil'ev, A. I. Valishev, V. A. Vasil'ev, and L. V. Panfilova, Characteristics of combustion and detonation of hydrazine and its methyl derivatives, *Fiz. Goreniya Vzryva*, **36**, No. 3, 81–96 (2000).
27. H. Matsui and J. H. Lee, On the measure of the relative detonation hazards of gaseous fuel-oxygen and air mixtures, in: *Proc. 17th Int. Symp. on Combust.*, 1269–1280 (1978).

28. R. Knystautas, C. Guirao, J. H. Lee, and A. Sulmistras, Measurement of cell size in hydrocarbon-air mixtures and predictions of critical tube diameter, critical initiation energy and detonation limits, in: J. R. Bowen, N. Manson, A. K. Oppenheim, and R. I. Soloukhin (Eds.), *Dynamics of Shock Waves, Explosions and Detonations, Progress in Astronautics and Aeronautics*, Vol. 94, New York (1983), pp. 23–37.
29. A. A. Vasil'ev, On the influence of nitrogen on the parameters of multifront detonation, *Fiz. Goreniya Vzryva*, **34**, No. 1, 79–83 (1998).
30. D. C. Bull, I. E. Elsworth, and G. Hooper, Initiation of spherical detonation in hydrocarbon-air mixtures, *Acta Astronaut.*, **5**, 997–1008 (1978).
31. A. A. Vasil'ev, Critical conditions for initiation of cylindrical multifront detonation, *Fiz. Goreniya Vzryva*, **34**, No. 2, 114–120 (1998).
32. A. A. Vasil'ev and D. V. Zak, Detonation of gas jets, *Fiz. Goreniya Vzryva*, **22**, No. 4, 81–88 (1986).
33. A. A. Vasil'ev, Characteristic regimes of propagation of multifront detonation along a convex surface, *Fiz. Goreniya Vzryva*, **35**, No. 5, 86–92 (1999).
34. S. M. Kogarko, Investigation of pressure on the end of a tube in the case of nonstationary rapid combustion, *Zh. Tekh. Fiz.*, **28**, No. 9, 2041–2045 (1958).
35. A. A. Vasil'ev, Gaseous fuels and detonation hazards, *Combustion and Detonation: Proc. 28th Int. Conf. of Fraunhofer Institute of Chemical Technologies*, Karlsruhe, Germany (1997), pp. 50.1–50.14.
36. W. B. Benedick, C. M. Guirao, R. Knystautas, and J. H. Lee, Critical charge for direct initiation of detonation in gaseous fuel-air mixtures, in: J. R. Bowen, J.-C. Leyer, and R. I. Soloukhin (Eds.), *Dynamics of Explosion; Progress in Astronautics and Aeronautics*, Vol. 106, New York (1986), pp. 181–202.
37. A. A. Vasil'ev, Investigation of the critical initiation of gaseous detonation, *Fiz. Goreniya Vzryva*, **19**, No. 1, 121–131 (1983).
38. A. A. Vasil'ev, Estimation of the initiation energy of cylindrical detonation, *Fiz. Goreniya Vzryva*, **14**, No. 3, 154–155 (1978).
39. A. A. Vasil'ev, Yu. A. Nikolaev, and V. Yu. Ul'yanitskii, Critical energy of initiation of multifront detonation, *Fiz. Goreniya Vzryva*, **15**, No. 6, 94–104 (1979).
40. S. A. Zhdan and V. V. Mitrofanov, A simple model for calculating the energy of initiation of heterogeneous and gaseous detonation, *Fiz. Goreniya Vzryva*, **21**, No. 6, 98–103 (1985).
41. J. H. Lee, Initiation of gaseous detonation, *Ann. Rev. Phys. Chem.*, **28**, 75–104 (1977).
42. J. H. Lee and H. Matsui, A comparison of the critical energies for direct initiation of spherical detonations in acetylene–oxygen mixtures, *Combust. Flame*, **28**, 61–66 (1977).
43. J. H. Lee and K. Ramamurthi, On the concept of the critical size of a detonation kernel, *Combust. Flame*, **27**, 331–340 (1976).
44. V. I. Makeev, Yu. A. Gostintsev, V. V. Stroganov, Yu. A. Bokhon, Yu. N. Chernushkin, and V. N. Kulikov, Combustion and detonation of hydrogen–air mixtures in free volumes, *Fiz. Goreniya Vzryva*, **19**, No. 5, 16–18 (1983).
45. V. A. Levin, V. V. Markov, and S. F. Osinkiv, Initiation of detonation in a hydrogen–air mixture by explosion of a spherical TNT charge, *Fiz. Goreniya Vzryva*, **31**, No. 2, 91–95 (1995).
46. S. M. Kogarko, V. V. Adushkin, and A. G. Lyamin, Investigation of the spherical detonation of gaseous mixtures, *Nauch. Tekh. Probl. Gor. Vzryva*, No. 2, 22–34 (1965).
47. R. Atkinson, D. C. Bull, and R. I. Shuff, Initiation of spherical detonation in hydrogen–air, *Combust. Flame*, **39**, 287–300 (1980).